

Estimation of Mangrove Gross Primary Productivity Using Sentinel-2 Imagery Data: A Case Study in Ujung Pangkah East Java, Indonesia

Zainul Hidayah^{1*}, Abd Rahman As-Syakur^{2,3}, Herlambang Aulia Rachman¹, Linda Sri Rahayu Romadhoni¹ and Martiwi Diah Setiawati⁴

¹Department of Marine Science and Fisheries, Faculty of Agriculture Trunojoyo University of Madura, Raya Telang 02 Madura East Java, 69162 Indonesia

²Department of Marine Science, Faculty of Marine and Fisheries, Udayana University Bukit Jimbaran Campus Bali, 80361 Indonesia

³Centre for Remote Sensing and Ocean Science (CReSOS) Udayana University Bali, 80361 Indonesia

⁴Institute for the Advanced Study of Sustainability (UNU-IAS), United Nations University, Tokyo, 150-8925 Japan

ABSTRACT

Mangrove forests are the main carbon absorption and sequestration source, serving as a typical ecosystem in coastal areas. Despite numerous studies on temporal changes in carbon storage, there is limited information on the examination of gross primary productivity (GPP) in mangrove forests. GPP is the overall quantity of organic matter produced in the vegetation through photosynthesis, including the portion used for respiration. In the context of global warming and climate change, GPP is frequently used as an indicator of the total amount of carbon dioxide (CO₂) assimilated by the ecosystem, particularly vegetation. The advancement of geographic information systems (GIS)

and remote sensing methods has enabled the estimation of GPP rates on a spatial-temporal basis. Therefore, this study aimed to estimate and explore the relationship between GPP and vegetation density in the mangrove forest of Ujung Pangkah, Indonesia. Multi-temporal Sentinel-2 image data from 2018 to 2022 were used for analysis, while the Vegetation Production Model (VPM) was applied to calculate GPP. The results showed a steady increase in average GPP from 1997.91 grC m⁻² yr⁻¹ in 2018 to 2290.09 grC m⁻² yr⁻¹ in 2022. The increase showed significant improvement in the condition of the Ujung Pangkah mangrove forest.

ARTICLE INFO

Article history:

Received: 16 April 2024

Accepted: 24 December 2024

Published: 07 March 2025

DOI: <https://doi.org/10.47836/pjst.33.2.12>

E-mail addresses:

zainulhidayah@trunojoyo.ac.id (Zainul Hidayah)

ar.assyakur@pplh.unud.ac.id (Abd Rahman As-syakur)

herlambang.rachman@trunojoyo.ac.id (Herlambang Aulia Rachman)

linda.rahayu@trunojoyo.ac.id (Linda Sri Rahayu Romadhoni)

martiwidiah@unuias.ac.id (Martiwi Diah Setiawati)

* Corresponding author

This was further confirmed by the strong relationship between GPP and the Normalized Difference Vegetation Index (NDVI), which was used to determine vegetation density ($R^2 > 0.9$, $p < 0.05$).

Keywords: Gross primary productivity, mangrove, photosynthesis, Sentinel-2, Ujung Pangkah

INTRODUCTION

Global warming is the catalyst for climate change, negatively affecting land and marine environments. This phenomenon causes high sea surface temperatures, changes in rainfall patterns, extreme weather conditions, and cyclonic storms. The most concerning increase in emissions is carbon dioxide (CO₂) due to higher concentration and long lifetime in the atmosphere. According to a recent World Meteorological Organization (WMO) report, the global atmospheric CO₂ concentration has reached a new high record of 415.7 ± 0.2 ppm in 2021 (Tang et al., 2023). On average, the increase in global CO₂ concentration in the last 2 decades is approximately 2.25 ppm/year (Friedlingstein et al., 2022). This continuous increase is significantly attributed to uncontrolled consumption of fossil fuels and massive land cover changes (Ayompe et al., 2020; Basu et al., 2020; Goldstein et al., 2020; Yoro & Daramola, 2020). The mangrove ecosystem has been proven effective due to its high carbon storage capacity.

The mangrove ecosystem is estimated to have five times the carbon storage capacity of terrestrial rainforest per hectare (Donato et al., 2011), with an optimal carbon sequestration function of approximately 77.9% (Chatting et al., 2022). Furthermore, high productivity combined with slow soil decay rates improves the ability to capture and preserve organic carbon (Alongi, 2012; Kauffman & Bhomia, 2017; Bacar et al., 2023; Hidayah et al., 2022). Indonesia has approximately 2.95 million ha of mangrove forest, accounting for 20.09% of the world's mangrove area (Bunting et al., 2022).

Although mangrove forests play significant ecological roles in coastal environments, this ecosystem is under threat from illegal logging, deforestation, and changes in land use. According to the United Nations Statistics geographic regions, the estimated extent of mangroves worldwide in 1996 was 15.26 million ha. In 2020, deforestation decreased to 14.73 million ha, with a rate of mangrove loss of 37,464 ha/year. During this period, the area of mangroves in Indonesia decreased by over 174,000 ha, from 3.12 million ha in 1996 to 2.95 million ha in 2020 (Bunting et al., 2022). Further studies showed that 70% of mangroves capable of producing organic compounds were deforested, and 30% were degraded (Hidayah et al., 2022; Bunting et al., 2022).

In this context, primary productivity is essential for the formation of energy-rich organic compounds from inorganic compounds. Gross and net primary productivity are both components of primary productivity. Net Primary Productivity (NPP) is the amount of primary productivity that remains after being used by organisms for respiration. Meanwhile, Gross Primary Productivity (GPP) is the total amount of organic compounds

formed in organism tissues during photosynthesis (Chapin et al., 2006; Wang et al., 2012). GPP is considered the total value of carbon fixation in terrestrial ecosystems through photosynthesis in a specific period, which is used to quantify the amount of CO₂ assimilated by vegetation (Nuarsa et al., 2018), particularly in mangrove ecosystems (Wang et al., 2012).

Several studies have been carried out on temporal changes and carbon stocks in mangrove biomass and sediment in Indonesia (Cameron et al., 2019; Harefa et al., 2022; Lukman et al., 2022; Pricillia et al., 2021; Trissanti et al., 2022). Allometric equations are commonly used to calculate carbon stocks in mangrove biomass (Hidayah et al., 2022; Indrayani et al., 2021; Suardana et al., 2023), with the regular procedure dependent on biophysical measurements. These include tree diameter at breast height, tree height, or wood density of various plant species, thereby limiting extrapolation to regional scales. This study used a combination of GIS and remote sensing methods to estimate GPP over time through the relationship with the fraction of absorbed photosynthetically active radiation (f-APAR) driven by vegetation indexes (Nuarsa et al., 2018). According to previous studies, the Moderate-resolution Imaging Spectroradiometer (MODIS) data were used to calculate GPP on vast terrestrial and coastal forest ecosystems (Kanniah et al., 2021; Turner et al., 2003). Landsat data were more frequently used for the estimation of other land cover types (Celis et al., 2023; Nuarsa et al., 2018; Raj et al., 2020; Shirkey et al., 2022). Therefore, this study aimed to estimate the GPP of Ujung Pangkah in East Java, Indonesia, using Sentinel-2 satellite data from 2018 to 2022. The analysis focused on three main objectives: to measure the change in the mangrove area. Second, analysis was conducted to estimate Ujung Pangkah's annual GPP using VPM, and third, to investigate the relationship between GPP and vegetation density.

MATERIAL AND METHODS

Study Location

Ujung Pangkah mangrove forest is located at the estuary of Bengawan Solo River, one of the longest and largest rivers in Indonesia. Geographically, this study area is located on Java Island's north coast, in the administrative area of Gresik Regency, East Java Province, as shown in Figure 1. Since 2021, Indonesia's Ministry of Environment and Forestry has designated this location as an Essential Ecosystem Area. The initiative is part of the Indonesian government's efforts to preserve wetland areas as defined by the Ramsar Convention, a UN-initiated intergovernmental convention for wetland conservation. Ujung Pangkah is located close to Gresik City, which is one of the largest industrial areas in Eastern Indonesia. This shows that factory operations in the area may emit excessive CO₂ into the atmosphere daily. Therefore, there is a need for more carbon-absorbing areas to balance the atmospheric carbon cycle.

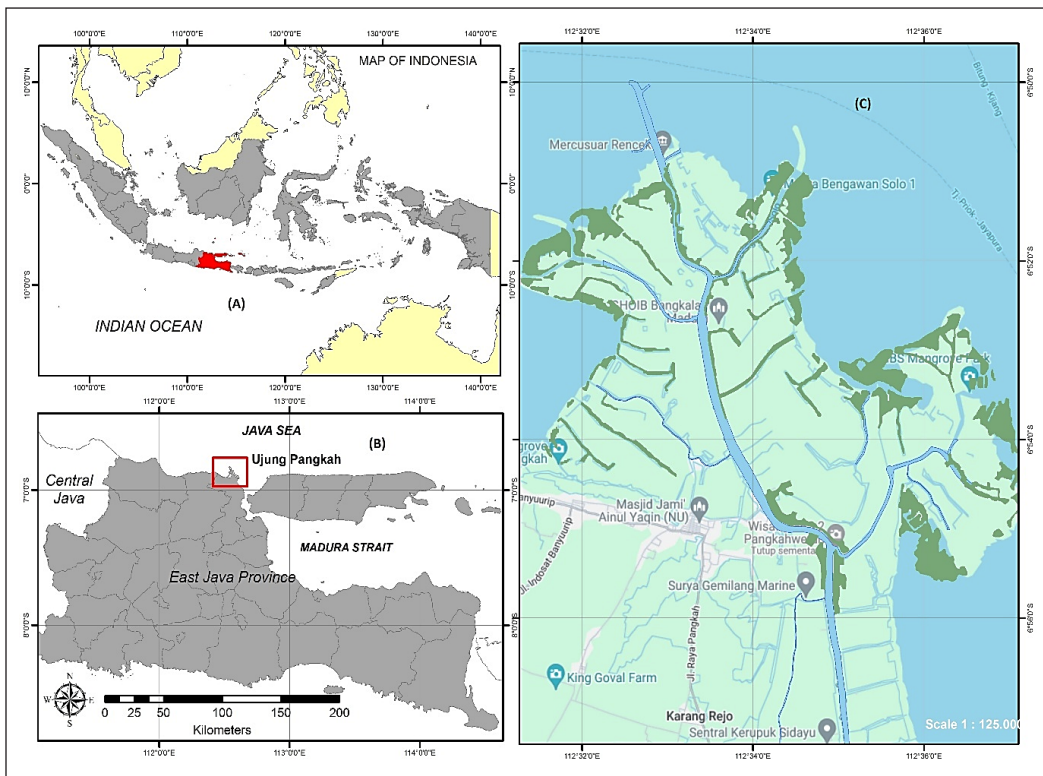


Figure 1. Study site: (A) East Java Province of Indonesia, (B) The location of Ujung Pangkah in East Java Province, (C) Coastal study sites in Ujung Pangkah with mangrove forests extracted from Sentinel-2 image

Data Description

The primary data used in this study was a set of multi-spectral Sentinel-2 Level 1C satellite images acquired from 2018 to 2022. These images were collected using the Google Earth Engine (GEE) platform <https://developers.google.com/earth-engine/datasets/catalog/sentinel>. European Space Agency (ESA) administered this satellite under the Copernicus Land Monitoring project. Sentinel-2 comprised two satellites with similar characteristics (Sentinel 2A and 2B), each equipped with a 13-band MSI (Multi-Spectral Instrument) optical sensor that covers the visible light to infrared spectrum. Every Sentinel-2 image covered a 290-kilometer strip, combined with its spatial resolution of 10 to 60 meters per pixel and 15 days of temporal resolution (Table 1).

Image processing was performed using the cloud computing platform GEE, accessible at <https://earthengine.google.com>. The investigation used a Sentinel-2 harmonized dataset, which included Surface Reflectance (SR) values. Annually, the analysis used composites obtained from data gathered from June to October, which was consistent with the dry season characterized by low cloud cover. Initially, only images that had a cloud cover of less than 30% were selected. Median composites were created by averaging the values of

Table 1
Spectral and spatial characteristics of Sentinel-2 imagery data

Bands	Wavelength (μm)	Spatial Resolution (m)
Band-1 Coastal Aerosol	0.433–0.453	60
Band 2: Blue	0.458–0.523	10
Band 3: Green	0.543–0.578	10
Band 4: Red	0.650–0.680	10
Band 5: Vegetation Red Edge	0.698–0.713	20
Band 6: Vegetation Red Edge	0.733–0.748	20
Band 7: Vegetation Red Edge	0.765–0.785	20
Band 8: NIR	0.758–0.900	10
Band 8A: Vegetation Red Edge	0.855–0.875	20
Band 9: Water Vapour	0.930–0.950	60
Band 10: SWIR Cirrus	1.365–1.385	60
Band 11: SWIR	1.565–1.655	20
Band 12: SWIR	2.100–2.280	20

Source: Sentinel-2 User's Guide (<https://sentinels.copernicus.eu/web/sentinel/user-guides/sentinel-2-msi/overview>)

each band over the complete dataset during this period. The method was used to mitigate the influence of cloud cover before categorization and subsequent analysis. Furthermore, this study used local monthly average temperature data from the meteorological station BMKG (Meteorological, Climatological, and Geophysical Agency) Sangkapura, available at https://dataonline.bmkg.go.id/data_iklim. Monthly sun radiation statistics data were also acquired from the European Centre for Medium-Range Weather Forecasts (ECMWF), accessible at <https://developers.google.com/earth-engine/datasets/catalog>.

Gross Primary Productivity (GPP) Calculation

Empirical models, such as the Satellite-based Light-Use Efficiency (LUE), are used to estimate GPP due to the challenges associated with direct measurement. According to the LUE model, carbon exchange can be determined through the quantity of light energy absorbed by vegetation and the effectiveness of converting carbon (Xiao et al., 2005). Vegetation Production Model (VPM) is one of the LUE models commonly used to estimate GPP based on remote sensing image data as well as the effects of temperature, water stress, and phenology. In VPM, three sets of parameters, namely light temperature parameters (T-scalar), water parameters (W-scalar), and leaf phenology (P-scalar), are used to estimate GPP (Xiao et al., 2005). Previous studies have confirmed the accuracy of GPP calculations derived from satellite image data using VPM estimation. The results show a strong correlation with CO₂ eddy flux towers, a widely used micro-meteorological method that measures the vertical concentration gradients of Green House Gases (GHGs) continuously (Huang et al., 2022; Kumar et al., 2017; Peddinti et al., 2020). Details of

Sentinel-2 image processing using GEE to calculate mangrove area and estimate annual GPP are systematically presented in Figure 2.

Sentinel-2 Image Processing

This study analyzed satellite images to acquire the remote sensing indexes required for calculating GPP. Initially, the pre-processing stage included using the GEE platform to mask clouds and perform rectification. This was followed by the computation of the Normalized Difference Vegetation Index (NDVI), Enhanced Vegetation Index (EVI), and Land Surface Water Index (LSWI). NDVI was used to differentiate mangrove vegetation from other forms of land cover. This vegetation index was computed using the proportion of near-infrared (NIR) of band eight and the red spectrum of band four from the Sentinel-2 image. The following Equation 1 was used to compute NDVI from image data.

$$NDVI = \frac{Nir - Red}{Nir + Red} \quad [1]$$

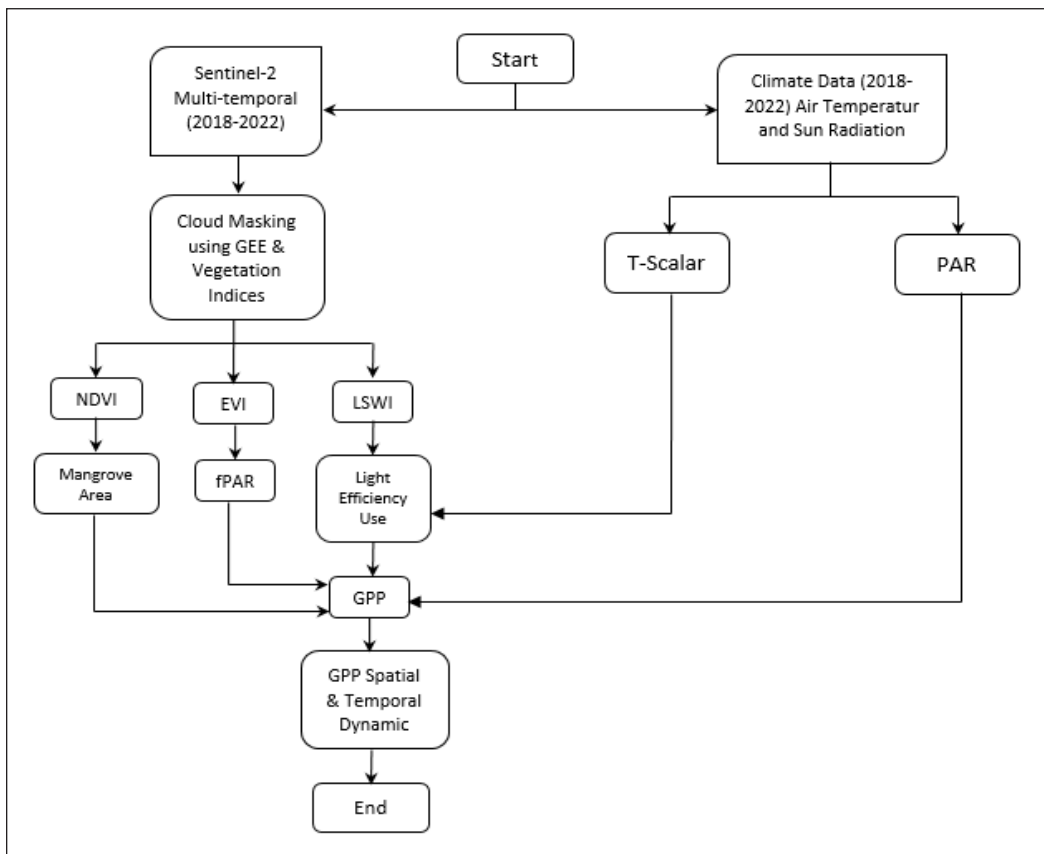


Figure 2. Flow chart of GPP data analysis using Vegetation Photosynthesis Model (VPM)

EVI was used due to the linear relationship with the leaf green index derived from multi-spectral data and the ability to determine changes in the cover of plants (Xiao et al., 2004). This index used a blue band to fix the atmosphere as well as blue, red, and NIR bands to observe the changing reflectance of soil and the canopy background (Nuarsa et al., 2018). Subsequently, EVI was calculated using three specific bands from Sentinel-2, including NIR (band 8), red (band 4), and blue (band 2). The values of EVI varied from -1 to +1, which was calculated using Equation 2 provided by Huete et al. (1997).

$$EVI = 2.5 \times \frac{\rho_{nir} - \rho_{red}}{\rho_{nir} + (6 \times \rho_{red} - 7.5 \times \rho_{blue}) + 1} \quad [2]$$

An additional index required for VPM, LSWI, was calculated using NIR (band 8) and SWIR (band 11) of the Sentinel-2 image. Increasing the amount of water in the leaf or the moisture in the soil led to greater absorption of shortwave infrared (SWIR) light and reduced reflection of NIR light. The value of LSWI ranged from -1 to +1, calculated using Equation 3 provided by Xiao et al. (2005).

$$LSWI = \frac{\rho_{nir} - \rho_{swir}}{\rho_{nir} + \rho_{swir}} \quad [3]$$

Vegetation Production Model (VPM)

In VPM, the T-scalar parameter was used to determine photosynthesis temperature using the Terrestrial Ecosystem Model (Equation 4) (Raich, 1991):

$$T - scalar = \frac{(T - T_{min}) \times (T - T_{maks})}{[(T - T_{min}) \times (T - T_{max})] - (T - T_{opt})^2} \quad [4]$$

The terrestrial ecosystem model measured the temperature for photosynthesis, often known as Tscalar, in degrees Celsius (°C). At this point, T represents the mean monthly temperature obtained from the meteorological station BMKG Sangkapura. This study used the following settings for Tmin, Tmax, and Topt at 0°C, 48°C, and 28°C, respectively (Nuarsa et al., 2018). Additionally, the W-scalar parameter was applied to quantify the impact of water on vegetation photosynthesis, as stated by Nuarsa et al. (2018). The calculation of this parameter was derived from LSWI obtained from the analysis of the Sentinel-2 image, as shown in Equation 5.

$$W - scalar = \frac{1 + LSWI}{1 + LSWI_{max}} \quad [5]$$

The final parameter in VPM was P-scalar, a leaf phenology value used to evaluate the influence of leaf age on photosynthesis at the canopy level. The duration of the leaf

lifespan determined the P-scalar value. For a canopy dominated by leaves with a one-year life expectancy, P-scalar was calculated as a linear function of two distinct phases using Equation 6 provided by Xiao et al. (2005).

$$P - \text{scalar} = \frac{1 + LSWI}{2} \quad [6]$$

The next calculation was performed to determine light use efficiency (ϵg), which was the function of temperature (T_{scalar}), water effect on photosynthesis (W_{scalar}), and leaf phenology (P_{scalar}), as expressed in Equation 7 (Xiao et al., 2005). In Equation 7, $\epsilon 0$ is the maximum light use efficiency and is equal to 0.40 gC mol^{-1}

$$\epsilon g = \epsilon 0 \times T_{\text{scalar}} \times W_{\text{scalar}} \times P_{\text{scalar}} \quad [7]$$

Equation 8 uses incoming solar radiation (R) data to calculate the photosynthetic active radiation (PAR) in $\mu\text{mol}/\text{m}^2\text{sec}$. Equation 8 estimates that approximately 45% of solar radiation ($W \text{ m}^{-2}$) is transformed into PAR. Moreover, the final factor in determining GPP is F-PARchl, which represents the fraction of photosynthetic active radiation absorbed by chlorophyll. The VPM model assumes that F-PARchl in photosynthesis is a linear function of EVI, with a coefficient A set to 1 (Equations 8 and 9).

$$PAR = 0.45 \times R \quad [8]$$

$$fPARchl = EVI \times A \quad [9]$$

The VPM model developed to estimate GPP according to PAV (photosynthetically active vegetation) and NPV (non-photosynthetic vegetation) is determined using Equation 10 (Xiao et al., 2005).

$$GPP = \epsilon g \times fPARchl \times PAR \quad [10]$$

RESULTS AND DISCUSSION

Temporal Change of Mangrove Area

The use of multitemporal satellite images in this study is exceptionally beneficial to understanding the dynamics of change in the mangrove forest of Ujung Pangkah. As a coastal ecosystem, mangrove vegetation grows in response to temperature, humidity, rainfall, and sunlight intensity. This ecosystem can be influenced by coastal erosion, which naturally reduces the area of mangrove forests, while accretion or sedimentation contributes to increasing capacity.

This study used NDVI to identify mangrove land covers due to the ability to differentiate between vegetation and other types of land cover. The value ranged from -1

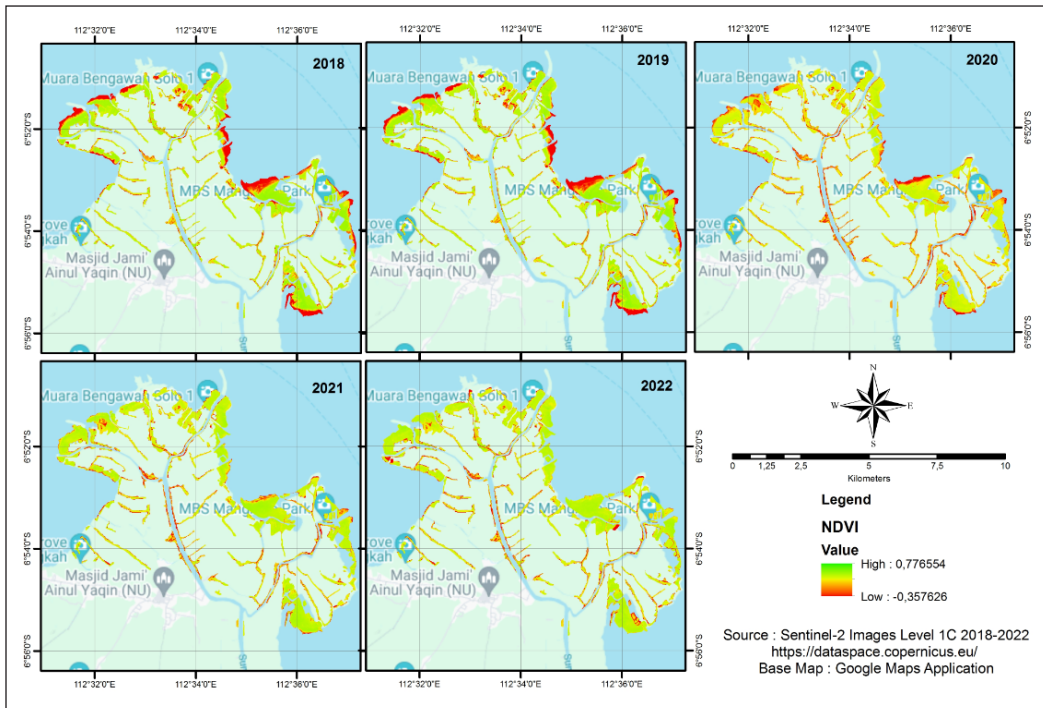


Figure 3. Distribution Map of Mangrove Forest of Ujung Pangkah East Java from 2018–2022

Table 2
Statistical parameters of NDVI and area of mangrove forest in Ujung Pangkah

Observation Year	NDVI Statistics				Total Area (Ha)
	Min	Max	Mean	Stdev	
2018	-0.32	0.61	0.48	0.25	1187.63
2019	-0.31	0.65	0.52	0.19	1217.21
2020	-0.25	0.70	0.48	0.17	1229.69
2021	-0.35	0.75	0.57	0.17	1239.24
2022	-0.35	0.77	0.56	0.17	1262.25

to 1, where vegetation was identified with $NDVI > 0$. Furthermore, using a supervised classification method, it was possible to identify mangrove vegetation based on unique growth patterns surrounding river estuaries. Figure 3 shows the map illustrating the distribution of mangroves in Ujung Pangkah.

According to the results of NDVI analysis in Table 2, the condition of the mangrove forest in Ujung Pangkah showed signs of enhancement during the past 5 years. This was supported by at least two indicators, including the expansion of mangrove coverage and the corresponding rise in average and maximum NDVI values. The area was 1187.63

Ha in 2018 and gradually increased to 1262.25 Ha by 2022, with the expansion strongly correlated to a high canopy density. Despite fluctuations in the average NDVI value, the maximum NDVI value gradually increased from 0.61 in 2018 to 0.77 in 2022.

The trend towards improving the condition of the mangrove forest ecosystem in Ujung Pangkah was supported by the position at Bengawan Solo estuary. The high rate of sedimentation in the year produced mud deposits rich in organic material, which served as a medium for vegetation growth. Suitable environmental conditions, as well as the absence of illegal logging or land conversion by local residents, played an important role in improving the condition of the mangrove ecosystem (Hagger et al., 2022). In recent years, the trend of expanding mangrove forest areas observed by medium-resolution satellite images was detected in several locations. These included Surabaya east coast and Teluk Pangpang of East Java, Indonesia; Thane Creek of Mumbai, India; than Hoa Estuary of Vietnam and Jiulong river estuary of China (Hidayah et al., 2022; Hidayah et al., 2024; Nguyen et al., 2020; Azeez et al., 2022; Wang et al., 2018).

Fluctuations in Yearly Temperature

Data on weather and environmental conditions at the research site were required to determine GPP using VPM. The annual temperature parameters obtained from Sangkapura weather station showed that from 2018 to 2022, the average annual air temperature in Ujung Pangkah mangrove forest ranged from 28.23°C to 28.53°C, with a small standard deviation of 0.46°C to 0.83°C. However, the average annual temperatures measured in the Ujung Pangkah mangrove forest area showed no significant difference (One Way ANOVA, $p > 0.05$, $df = 4$).

Figure 4 shows that the average annual temperature fluctuates over a 5-year period. The average annual temperature in 2018 was 28.50°C, which increased to 28.53°C in 2021 before decreasing to 28.36°C in 2022. Based on the results, 2018 had the smallest monthly temperature fluctuations ($\sigma = 0.46$), while the highest value occurred in 2020 ($\sigma = 0.83$). According to the Indonesian climate, the air temperature is often higher during the peak of the dry season, which occurs between July and September, compared to the rainy season (February). These parameters, particularly air temperature, often influence the growth and formation of mangrove vegetation (Duke et al., 1998; Hutchison et al., 2014). Temperature is essential in physiological processes such as photosynthesis and respiration (Bernacchi et al., 2001). Therefore, optimum mangrove growth requires an average temperature of over 20°C and seasonal differences of no more than 5°C (Quisthoudt et al., 2012).

Estimation of Annual GPP

During the 5 years of observation, GPP calculations estimated using VPM produced distinctive results. At the start of observations in 2018, GPP in Ujung Pangkah mangrove

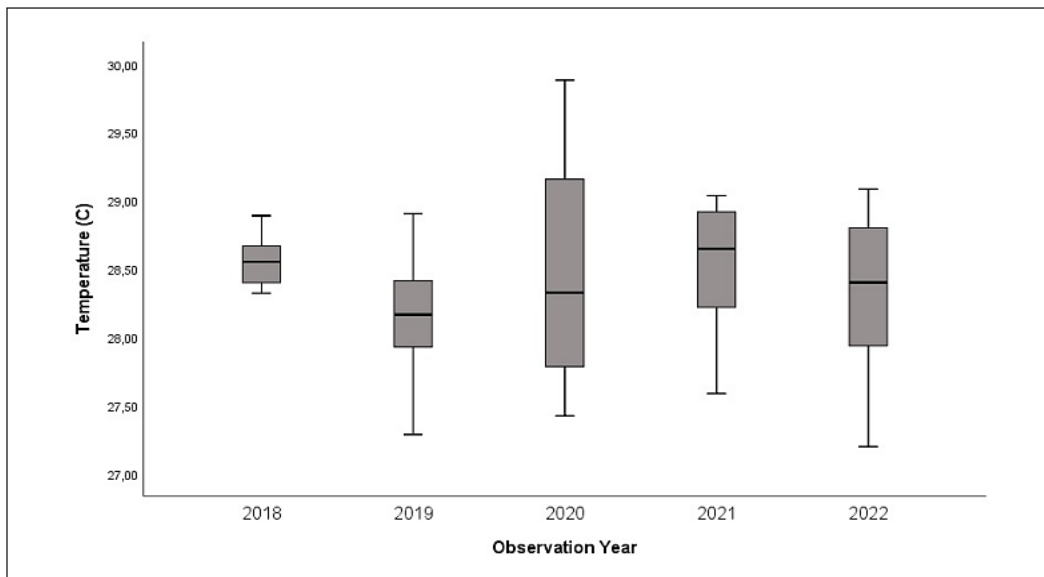


Figure 4. Monthly temperature fluctuations in the Ujung Pangkah mangrove forest area

forest ranged from $0.50 \text{ grC m}^{-2} \text{ yr}^{-1}$ to $4059.93 \text{ grC m}^{-2} \text{ yr}^{-1}$, with an average of $1997.90 \text{ grC m}^{-2} \text{ yr}^{-1}$. Meanwhile, in 2022, the final year of measurements, it ranged from $0.58 \text{ grC m}^{-2} \text{ yr}^{-1}$ to $4056 \text{ grC m}^{-2} \text{ yr}^{-1}$, with the average increase to $2290.09 \text{ grC m}^{-2} \text{ yr}^{-1}$.

The results showed that the expansion of the mangrove forest area directly impacted the rise in total (tC yr^{-1}). Table 3 shows the dynamics of changes in the GPP of the Ujung Pangkah mangrove forest, while spatial distribution based on Sentinel-2 image from 2018–2022 is presented in Figure 5. The increase in GPP can be attributed to the area’s improving mangrove ecosystem, which significantly contributes to high vegetation productivity, followed by canopy size and tree density growth. This phenomenon leads to improved Fraction of Absorbed Photosynthetically Active Radiation (fAPAR) and higher LUE, contributing to an increase in GPP (Zheng & Takeuchi, 2021).

During 5 years of observations using Sentinel-2 image, the Ujung Pangkah mangrove forest was dominated by areas with GPP in the range of $2401\text{--}3200 \text{ grC m}^{-2} \text{ yr}^{-1}$, covering 394.8 ha to 661.80 ha , or approximately $33.34\%\text{--}53.38\%$ of the total mangrove area each year. Meanwhile, areas with GPP in the range $3201\text{--}4010 \text{ grC m}^{-2} \text{ yr}^{-1}$ had the lowest percentage over the same period, ranging from 29.85% to 46.53% (Table 3). Based on Figure 5, changes in GPP occurred along the edges of the Ujung Pangkah mangrove forest, particularly to the east and north, which was predominantly dominated by GPP from 0.5 to $800 \text{ gr m}^{-2} \text{ yr}^{-1}$. 2018, the mangrove area with GPP 0.5 to $800 \text{ grC m}^{-2} \text{ yr}^{-1}$ was approximately 307.53 ha . In subsequent years, the area of mangroves with low GPP decreased, reaching 93.38 ha in 2022 (Table 4). Although not excessively large, the area

Table 3
Annual GPP of Ujung Pangkah mangrove forest from Sentinel-2 Images 2018–2022

Year	GPP (grC m ⁻² yr ⁻¹)				Total GPP (tC yr ⁻¹)
	Min	Max	Mean	Stdev	
2018	0.497	4053.97	1997.91	844.87	23.728
2019	0.655	3645.43	1909.96	796.96	23.248
2020	0.632	3547.94	2022.25	773.58	24.867
2021	0.978	3893.96	2137.87	746.15	26.493
2022	0.508	4056.06	2290.09	689.33	28.907

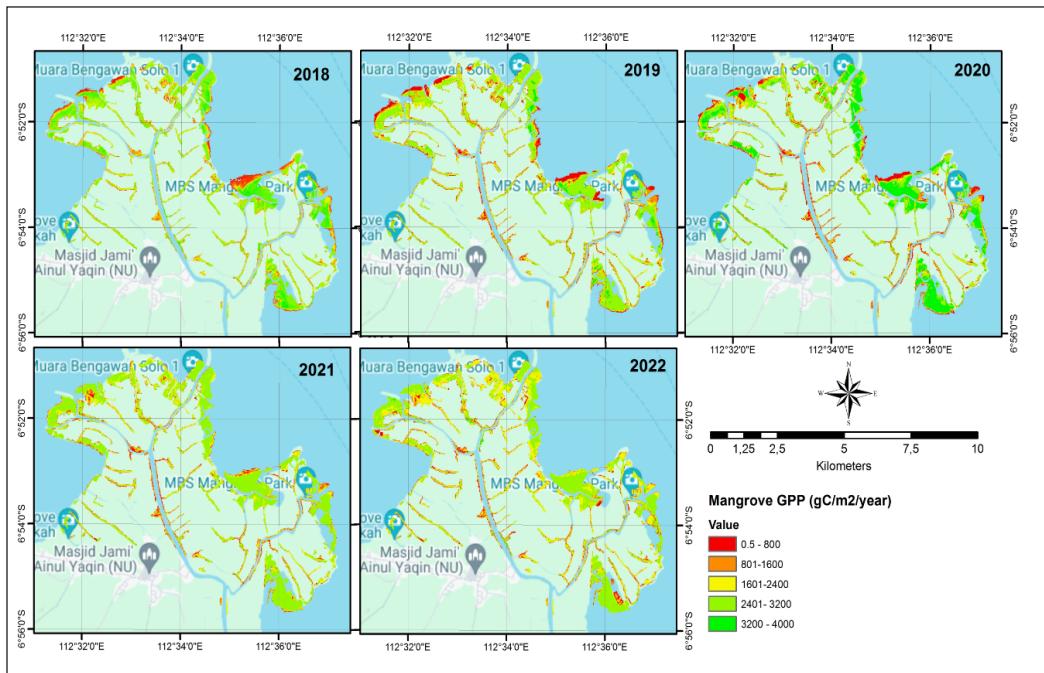


Figure 5. Annual GPP change in Ujung Pangkah mangrove forest East Java 2018–2022

Table 4
Total mangrove area covered based on GPP range

GPP Range (grC m ⁻² yr ⁻¹)	Mangrove Area (Ha)				
	2018	2019	2020	2021	2022
0.5–800	307.53	150.19	148.24	79.48	93.38
801–1600	158.86	173.46	183.43	143.86	149.58
1601–2400	291.4	305.27	353.51	308.94	438.46
2401–3200	394.8	552.96	501.31	661.8	536.08
3201–4010	29.85	35.92	42.93	45.62	46.53
Total	1185.44	1217.8	1229.42	1239.7	1264.83

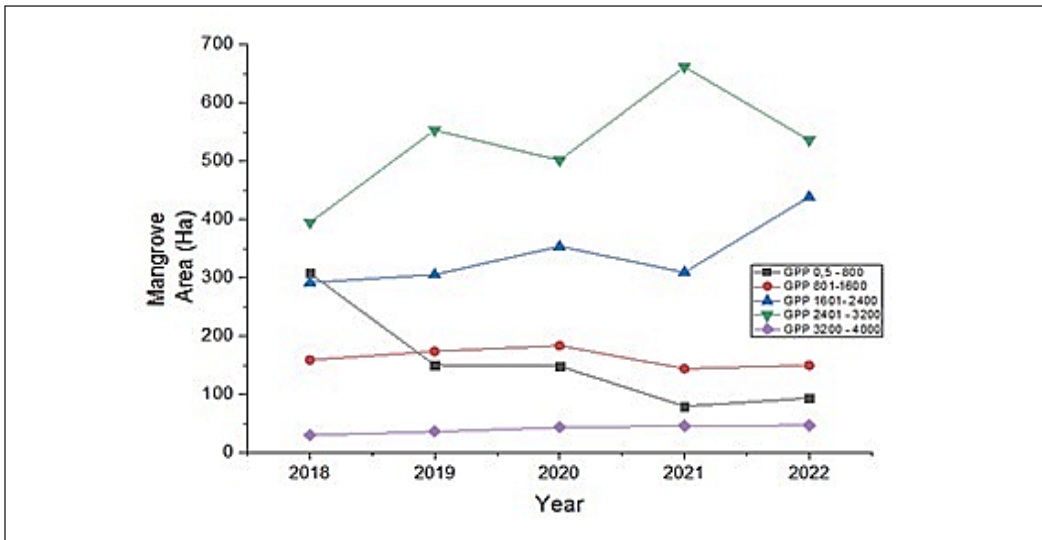


Figure 6. The dynamic of mangrove area based on GPP of Ujung Pangkah mangrove forest

of mangrove forest with the highest GPP interval in this study (3201–4010 grC m⁻² yr⁻¹) increased from 29.85 ha (2.58% of the total area) in 2018 to approximately 46.53 ha (3.68%) in 2022. The estimation of GPP provided information about mangrove health in terms of photosynthetic efficiency and carbon sequestering (Kumar & Das, 2023). Further investigation confirmed a clear indication of improvements in the mangrove health of Ujung Pangkah. The phenomenon was observed by a consistent decrease in mangrove area with GPP in low intervals, namely 0.5–800 grC m⁻² yr⁻¹ and 801–1600 grC m⁻² yr⁻¹. This was followed by an increase in GPP at higher intervals, namely 1601–2400 grC m⁻² yr⁻¹ and 3201–4010 grC m⁻² yr⁻¹, respectively (Figure 6).

Several studies have emphasized GPP as an essential parameter in the assessment of the global carbon budget of mangrove ecosystems (Beer et al., 2010; Alongi, 2014; Zheng & Takeuchi, 2022). Presently, the primary methods for determining forest GPP include direct observations, flux tower methods, and remote sensing models. The direct measuring method assesses leaf photosynthesis within a controlled laboratory setting. However, it is impractical to quantify the gross primary productivity (GPP) of forests across extensive areas (Zhao et al., 2023). The flux tower approach quantifies the exchange of carbon dioxide (CO₂) between ecosystems and the atmosphere by employing eddy correlation (EC) techniques. This method requires the collection of continuous observation data. Nonetheless, the number of operational flux tower sites is currently limited, and they have limited availability over the globe (Wang et al., 2019; Gnanamoorthy et al., 2020). The estimation of GPP using remote sensing data depends on the light-use efficiency (LUE) under various environmental circumstances and ecosystem structures (Z. Zhang et al., 2023). Additionally, global or regional GPP estimations can be derived from site-level

GPP observations through spatial extrapolation using remote sensing models (Huang et al., 2019; Markiet & Mottus, 2020; Y. Zhang et al., 2023).

Utilizing remote sensing techniques to implement modeled GPP has the potential to enhance and expand the investigation of carbon processes in mangroves on a larger scope. A comparison of the modeled GPP with in-situ flux tower data is required to assess its validity. Due to the absence of flux tower data near the location of this study, the comparison cannot be done. However, the GPP estimation of this study in the Ujung Pangkah mangrove forest was not significantly different and remained within the confidence interval of measurement results obtained from flux-tower measurements in multiple locations; for example, GPP measurements in Zhangjiang, China, reported an average result of $1729 \text{ grC m}^{-2} \text{ yr}^{-1}$ to $1924 \text{ grC m}^{-2} \text{ yr}^{-1}$ (Li et al., 2015). Meanwhile, GPP measurements in India's Picharam mangrove forest revealed slightly higher results, around $2305 \text{ grC m}^{-2} \text{ yr}^{-1}$ (Gnanamoorthy et al., 2020). However, measurements in the Sunderbans obtained lower results of $1271 \text{ grC m}^{-2} \text{ yr}^{-1}$ (Rodda et al., 2016).

Variations in GPP estimates across sites could be attributed to differences in climate-hydrological conditions, mangrove species, and age (Li et al., 2015). Meanwhile, several factors influenced these variations at the same site, including forest vegetation structure and stand parameters such as stem size, canopy cover, basal area, leaf area index, and vegetation density (Kanniah et al., 2021). Several studies also reported that specific environmental variables such as high salinity and extremely low temperatures could limit GPP (Inoue et al., 2022; Krauss et al., 2008; Reef & Lovelock, 2015).

Relationship Between NDVI and GPP

Further analysis was conducted to determine the relationship between mangrove NDVI and GPP. Moreover, NDVI was selected over other vegetation indexes because of its wide application to estimate mangrove forest density based on canopy cover (Razali et al., 2020; Zaitunah et al., 2021; Zhao & Qin, 2020). Despite accuracy issues caused by weather disturbances, satellite movement, and zonal peak angle, which interfered with the vegetation canopy reflectance response signal (Rafique et al., 2016), NDVI was extensively used to understand the spatiotemporal pattern of vegetation cover change (Kaufmann et al., 2003; Wang et al., 2021). This study modeled the relationship between NDVI and GPP using linear regression (Figure 7).

Based on the regression model, NDVI had a significant influence on GPP. This was explained by the consistency of linear regression results across observation years, with a coefficient of determination (R^2) greater than 0.90, indicating that NDVI showed an adequate indicator for estimating GPP. Vegetation indexes, such as NDVI, were used in multi-channel image processing to show aspects of vegetation density or other density-related characteristics, such as biomass and chlorophyll concentration. A high vegetation

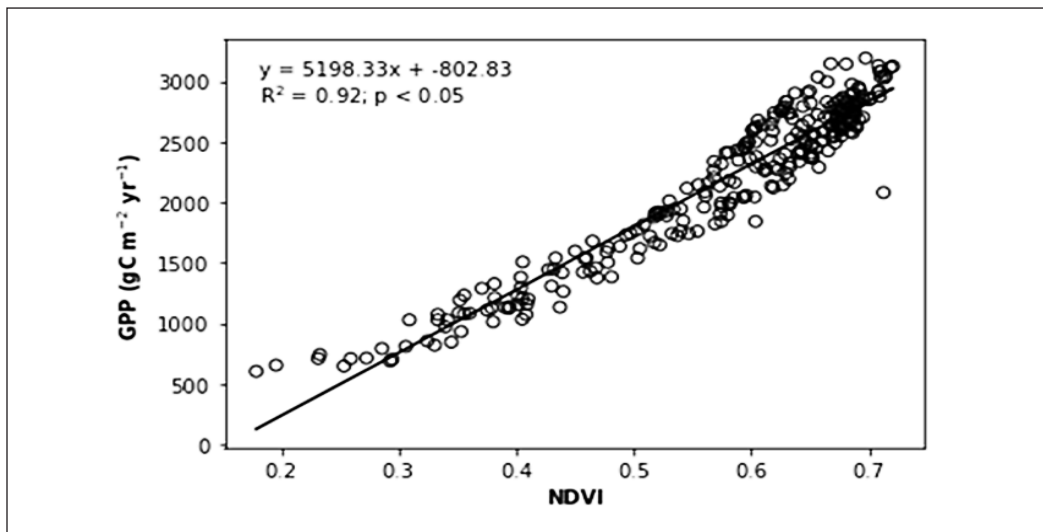


Figure 7. Linear regression models NDVI and GPP of Ujung Pangkah mangrove forest

index value showed that the area under observation had elevated levels of greenness, such as dense forest areas. Meanwhile, a low vegetation index value showed a decrease in vegetation greenness and cover.

It is noteworthy that GPP has more direct relations to the photosynthesis rate, leaves, and biomass growth. In relation to GPP, NDVI primarily indicates vegetation coverage and chlorophyll content without a direct relationship to vegetation photosynthesis as the primary parameter in the LUE model used to calculate GPP in this study. Many studies have discovered that biophysical conditions have a significant impact on NDVI in mangrove ecosystems (Alongi, 2022; Hidayah et al., 2022; Lukman et al., 2022; Hidayah et al., 2024). Furthermore, NDVI in mangroves provides a comprehensive view of ecosystem conditions. Accordingly, NDVI trends fluctuate in response to meteorological factors, such as temperature and precipitation (Ichii et al., 2022). Given the positive results of this study in modeling the relationship between NDVI and GPP, it can be argued that spatial and temporal changes in NDVI can be used as an observational proxy for studying global, regional, and temporal changes in GPP.

Previous studies discovered that biophysical conditions had a significant impact on NDVI in mangrove ecosystems (Alongi, 2022; Hidayah et al., 2022; Lukman et al., 2022; Hidayah et al., 2024). Moreover, NDVI trends fluctuate in response to meteorological factors, such as temperature and precipitation (Ichii et al., 2022). Based on the positive results, it was discovered that spatial and temporal changes in NDVI could be used as an observational proxy for exploring global, regional, and temporal changes in GPP.

The gross amount of organic matter produced by mangroves indicated the ability to absorb atmospheric CO₂ and convert it to biomass through photosynthesis. Discovering the

spatial and temporal variations of GPP in mangroves is crucial for accurately estimating the capacity of coastal ecosystems to store carbon. Climate conditions, vegetation types, and their spatial distribution, as well as factors that influence mangrove distribution, such as land-use practices and land cover conversion, primarily control spatial variations of GPP. Similarly, the seasonal phenology of vegetation and climate conditions influence the temporal variations of GPP (Cao et al., 2004; Nemani et al., 2003).

The Importance of Mangrove GPP in Global Carbon Studies

The significance of studying the contribution of mangrove forests to carbon sequestration is heightened when considering the implications of global warming and climate change. Industrialized countries with high carbon emissions are strongly believed to be a major cause of global warming, which poses a significant threat to environmental sustainability and human well-being (Alongi, 2020). In order to proactively address the issue of global warming, numerous governments have implemented carbon-neutral policies that are centered around the concept of carbon reduction (Huang & Zhai, 2021; Chen et al., 2022). China has declared its climate objectives, which include reaching the peak of carbon emissions by 2030 and achieving carbon neutrality by 2060 (Zeng et al., 2022), whereas the European Union has set its goal of carbon neutrality by 2050 (Perissi & Jones, 2022).

Blue carbon ecosystems (BCEs), which encompass mangrove forests, seagrass meadows, and tidal marshes, serve as carbon sinks and offer additional advantages, including protecting the coastline and improving fisheries. BCE sequestration is proposed as a natural system to address climate change and prevent the further impact of global warming (Hilmi et al., 2021; Mengis et al., 2023). On a global scale, BCEs have an estimated carbon storage capacity of around 30,000 Tg C and conserving these ecosystems prevents annual emissions of 141-466 Tg CO₂ equivalent (CO₂e) (Macreadie et al., 2021). It is imperative that mangrove forests provide an essential function in the global carbon cycle; therefore, accurately estimating carbon stock and release to comprehend the carbon budget in BCEs is vital (Zhao et al., 2023).

In this regard, mangrove GPP studies, which can reflect the capacity of carbon capture and sequestration potential by coastal vegetation, play an important role. Properly estimating GPP in mangrove forests is vital for monitoring and evaluating the growth of vegetation, carbon balance, and carbon conversion (Zhu et al., 2021; Paramanik et al., 2022). In addition, GPP studies offer extensive significance in surveilling the terrestrial carbon cycle and determining the magnitude of carbon sources and sinks in the Earth system (Bertram et al., 2021; Zhu et al., 2021). Hence, by monitoring the spatial and temporal patterns of GPP, changes in the carbon budget at a regional level can be determined. This information can then be used as a scientific foundation for creating policies that aim to address climate adaptation and achieve carbon neutrality objectives.

CONCLUSION

In conclusion, this study showed the use of Sentinel-2 image to estimate GPP in the mangrove forest of Ujung Pangkah, East Java, Indonesia. The results showed a significant increase in mangrove area, from 1187.63 ha in 2018 to approximately 1262.25 ha in 2022. This improvement has had a positive impact on mangroves' ability to absorb carbon, as shown by an increase in average GPP from 1997.91 grC m⁻² yr⁻¹ to 2290.09 grC m⁻² yr⁻¹. Mangrove forest GPP fluctuations over time were determined by vegetation density. This was confirmed by the positive relationship between GPP and NDVI, which measured mangrove vegetation density through satellite image processing ($R^2 > 0.9$, $p < 0.05$). This study also emphasized that the application of remote sensing and GIS has the potential to improve and broaden the study of carbon dynamics, particularly GPP in mangrove forests, on a larger scale.

ACKNOWLEDGEMENT

This work was supported by funding from the Institute of Research and Community Development (LPPM) National Collaboration Scheme (University of Trunojoyo Madura and Udayana University) 2024.

REFERENCES

- Alongi, D. M. (2012). Carbon sequestration in mangrove forests. *Carbon Management*, 3(3), 313-322.
- Alongi, D. M. (2014). Carbon cycling and storage in mangrove forests. *Annual Review of Marine Science*, 6, 195-219.
- Alongi, D. M. (2020). Carbon balance in salt marsh and mangrove ecosystems: A global synthesis. *Journal of Marine Science and Engineering*, 8(10), Article 767. <https://doi.org/10.3390/jmse8100767>
- Alongi, D. M. (2022). Impacts of climate change on blue carbon stocks and fluxes in mangrove forests. *Forests*, 13(2), Article 149. <https://doi.org/10.3390/f13020149>
- Ayompe, L. M., Davis, S. J., & Egoh, B. N. (2020). Trends and drivers of African fossil fuel CO₂ emissions 1990-2017. *Environmental Research Letters*, 15(12), Article 124039. <https://doi.org/10.1088/1748-9326/abc64f>
- Azeez, A., Gnanappazham, L., Muraleedharan, K. R., Revichandran, C., John, S., Seena, G., & Thomas, J. (2022). Multi-decadal changes of mangrove forest and its response to the tidal dynamics of thane creek, Mumbai. *Journal of Sea Research*, 180, Article 102162.
- Bacar, F. F., Lisboa, S. N., & Siteo, A. (2023). The mangrove forest of Quirimbas National Park reveals high carbon stock than previously estimated in Southern Africa. *Wetlands*, 43(6), 1–15. <https://doi.org/10.1007/s13157-023-01707-1>
- Basu, S., Lehman, S. J., Miller, J. B., Andrews, A. E., Sweeney, C., Gurney, K. R., Xu, X., Southon, J., & Tans, P. P. (2020). Estimating US fossil fuel CO₂ emissions from measurements of 14C in atmospheric CO₂. *Proceedings of the National Academy of Sciences of the United States of America*, 117(24), 13300–13307. <https://doi.org/10.1073/pnas.1919032117>

- Beer, C., Reichstein, M., Tomelleri, E., Ciais, P., Jung, M., Carvalhais, N., Rödenbeck, C., Arain, M. A., Baldocchi, D., Bonan, G. B., Bondeau, A., Cescatti, A., Lasslop, G., Lindroth, A., Lomas, M., Luysaert, S., Margolis, H., Oleson, K. W., Rouspard, O., ... & Papale, D. (2010). Terrestrial gross carbon dioxide uptake: Global distribution and covariation with climate. *Science*, 329(5993), 834-838. <https://doi.org/10.1126/science.1184984>
- Bernacchi, C. J., Singaas, E. L., Pimentel, C., Portis, A. R., & Long, S. P. (2001). Improved temperature response functions for models of Rubisco-limited photosynthesis. *Plant, Cell & Environment*, 24(2), 253-259.
- Bertram, C., Quaas, M., Reusch, T. B., Vafeidis, A. T., Wolff, C., & Rickels, W. (2021). The blue carbon wealth of nations. *Nature Climate Change*, 11(8), 704-709. <https://doi.org/10.1038/s41558-021-01089-4>
- Bunting, P., Rosenqvist, A., Hilarides, L., Lucas, R. M., Thomas, N., Tadono, T., Worthington, T. A., Spalding, M., Murray, N. J., & Rebelo, L. M. (2022). Global mangrove extent change 1996–2020: Global mangrove watch version 3.0. *Remote Sensing*, 14(15), Article 3657. <https://doi.org/10.3390/rs14153657>
- Cameron, C., Hutley, L. B., Friess, D. A., & Brown, B. (2019). Community structure dynamics and carbon stock change of rehabilitated mangrove forests in Sulawesi, Indonesia. *Ecological Applications*, 29(1), Article e01810. <https://doi.org/10.1002/eap.1810>
- Cao, M., Prince, S. D., Small, J., & Goetz, S. J. (2004). Remotely sensed interannual variations and trends in terrestrial net primary productivity 1981–2000. *Ecosystems*, 7, 233–242. <https://doi.org/10.1007/s10021-003-0189-x>
- Celis, J., Xiao, X., White, P. M., Cabral, O. M. R., & Freitas, H. C. (2023). Improved modeling of gross primary production and transpiration of sugarcane plantations with time-series Landsat and Sentinel-2 images. *Remote Sensing*, 16(1), Article 46. <https://doi.org/10.3390/rs16010046>
- Chapin, F. S., Woodwell, G. M., Randerson, J. T., Rastetter, E. B., Lovett, G. M., Baldocchi, D. D., Clark, D. A., Harmon, M. E., Schimel, D. S., Valentini, R., Wirth, C., Aber, J. D., Cole, J. J., Goulden, M. L., Harden, J. W., Heimann, M., Howarth, R. W., Matson, P. A., McGuire, A. D., ... & Schulze, E. D. (2006). Reconciling carbon-cycle concepts, terminology, and methods. *Ecosystems*, 9(7), 1041–1050. <https://doi.org/10.1007/s10021-005-0105-7>
- Chatting, M., Al-Maslamani, I., Walton, M., Skov, M. W., Kennedy, H., Husrevoglu, Y. S., & Le Vay, L. (2022). Future mangrove carbon storage under climate change and deforestation. *Frontiers in Marine Science*, 9, 1–14. <https://doi.org/10.3389/fmars.2022.781876>
- Chen, L., Msigwa, G., Yang, M., Osman, A. I., Fawzy, S., Rooney, D. W., & Yap, P. S. (2022). Strategies to achieve a carbon neutral society: A review. *Environmental Chemistry Letters*, 20(4), 2277-2310. <https://doi.org/10.1007/s10311-022-01435-8>
- Donato, D. C., Kauffman, J. B., Murdiyarso, D., Kurnianto, S., Stidham, M., & Kanninen, M. (2011). Mangroves among the most carbon-rich forests in the tropics. *Natural Geoscience*, 4, 293–297.
- Duke, N. C., Ball, M. C., & Ellison, J. C. (1998) Factors influencing biodiversity and distributional gradients in mangroves. *Global Ecology Biogeography Letter*, 7(1),27–47. <https://doi.org/10.2307/299769>
- Friedlingstein, P., Jones, M. W., O’Sullivan, M., Andrew, R. M., Bakker, D. C. E., Hauck, J., Le Quééré, C., Peters, G. P., Peters, W., Pongratz, J., Sitch, S., Canadell, J. G., Ciais, P., Jackson, R. B., Alin, S. R.,

- Anthoni, P., Bates, N. R., Becker, M., Bellouin, N., ... & Zeng, J. (2022). Global Carbon Budget 2021. *Earth System Science Data*, 14(4), 1917–2005. <https://doi.org/10.5194/essd-14-1917-2022>
- Gnanamoorthy, P., Selvam, V., Burman, P. K. D., Chakraborty, S., Karipot, A., Nagarajan, R., & Grace, J. (2020). Seasonal variations of net ecosystem (CO₂) exchange in the Indian tropical mangrove forest of Pichavaram. *Estuarine, Coastal and Shelf Science*, 243, Article 106828. <https://doi.org/10.1016/j.ecss.2020.106828>
- Goldstein, A., Turner, W. R., Spawn, S. A., Anderson-teixeira, K. J., Cook-patton, S., Fargione, J., Gibbs, H. K., Griscom, B., Hewson, J. H., Howard, J. F., Ledezma, J. C., Page, S., Koh, L. P., Rockström, J., Sanderman, J., & Hole, D. G. (2020). Protecting irrecoverable carbon in Earth's ecosystems. *Nature Climate*, 10(4), 287–295. <https://doi.org/10.1038/s41558-020-0738-8>
- Hagger, V., Worthington, T. A., Lovelock, C. E., Adame, M. F., Amano, T., Brown, B. M., Friess, D. A., Landis, E., Mumby, P. J., Morrison, T. H., O'Brien, K. R., Wilson, K. A., Zganjar, C., & Saunders, M. I. (2022). Drivers of global mangrove loss and gain in social-ecological systems. *Nature Communications*, 13(1), 1–16. <https://doi.org/10.1038/s41467-022-33962-x>
- Harefa, M. S., Nasution, Z., Mulya, M. B., & Maksun, A. (2022). Mangrove species diversity and carbon stock in silvofishery ponds in Deli Serdang District, North Sumatra, Indonesia. *Biodiversitas*, 23(2), 655–662. <https://doi.org/10.13057/biodiv/d230206>
- Hidayah, Z., Rachman, H. A., & As-Syakur, A. R. (2022). Mapping of mangrove forest and carbon stock estimation of east coast Surabaya, Indonesia. *Biodiversitas*, 23(9), 4826–4837. <https://doi.org/10.13057/biodiv/d230951>
- Hidayah, Z., Utama, R. Y. S., As-Syakur, A. R., Rachman, H. A., & Wiyanto, D. B. (2024). Mapping mangrove above ground carbon stock of benoa bay bali using sentinel-1 satellite imagery. In *IOP Conference Series: Earth and Environmental Science* (Vol. 1298, No. 1, p. 012013). IOP Publishing. <https://doi.org/10.1088/1755-1315/1298/1/012013>
- Hidayah, Z., Rachman, H. A., & Wiyanto, D. B. (2024). Assessment of spatio-temporal dynamics of mangrove forest in Teluk Pangpang, Banyuwangi, East Java, Indonesia. *Biodiversitas: Journal of Biological Diversity*, 25(7), 3138–3150. <https://doi.org/10.13057/Biodiv/D250736>
- Hilmi, N., Chami, R., Sutherland, M. D., Hall-Spencer, J. M., Lebleu, L., Benitez, M. B., & Levin, L. A. (2021). The role of blue carbon in climate change mitigation and carbon stock conservation. *Frontiers in climate*, 3, Article 710546. <https://doi.org/10.3389/fclim.2021.710546>
- Huang, Q., Qiu, F., Fan, W., Liu, Y., & Zhang, Q. (2019). Evaluation of different methods for estimating the fraction of sunlit leaves and its contribution for photochemical reflectance index utilization in a coniferous forest. *Remote Sensing*, 11(14), Article 1643. <https://doi.org/10.3390/rs11141643>
- Huang, M. T., & Zhai, P. M. (2021). Achieving Paris Agreement temperature goals requires carbon neutrality by middle century with far-reaching transitions in the whole society. *Advances in Climate Change Research*, 12(2), 281–286. <https://doi.org/10.1016/j.accre.2021.03.004>
- Huang, X., Lin, S., Li, X., Ma, M., Wu, C., & Yuan, W. (2022). How well can matching high spatial resolution landsat data with flux tower footprints improve estimates of vegetation gross primary production. *Remote Sensing*, 14(23), Article 6062. <https://doi.org/10.3390/rs14236062>
- Huete, A. R., Liu, H. Q., Batchily, K. V., & Van Leeuwen, W. J. D. A. (1997). A comparison of vegetation indices over a global set of TM images for EOS-MODIS. *Remote Sensing of Environment*, 59(3), 440–451.

- Hutchison, J., Manica, A., Swetnam, R., Balmford, A., & Spalding, M. (2014). Predicting global patterns in mangrove forest biomass. *Conservation Letter*, 7(3), 233–240. <https://doi.org/10.1111/conl.12060>
- Ichii, K., Kawabata, A., & Yamaguchi, Y. (2002). Global correlation analysis for NDVI and climatic variables and NDVI trends: 1982-1990. *International Journal of Remote Sensing*, 23(18), 3873-3878. <https://doi.org/10.1080/01431160110119416>
- Indrayani, E., Kalor, J. D., Warpur, M., & Hamuna, B. (2021). Using allometric equations to estimate mangrove biomass and carbon stock in Demta Bay, Papua Province, Indonesia. *Journal of Ecological Engineering*, 22(5), 263–271. <https://doi.org/10.12911/22998993/135945>
- Inoue, T., Akaji, Y., & Noguchi, K. (2022). Distinct responses of growth and respiration to growth temperatures in two mangrove species. *Annals of Botany*, 129(1), 15–28. <https://doi.org/10.1093/aob/mcab117>
- Kanniah, K. D., Kang, C. S., Sharma, S., & Amir, A. A. (2021). Remote sensing to study mangrove fragmentation and its impacts on leaf area index and gross primary productivity in the south of peninsular malaysia. *Remote Sensing*, 13(8), Article 1427. <https://doi.org/10.3390/rs13081427>
- Krauss, K. W., Lovelock, C. E., McKee, K. L., López-Hoffman, L., Ewe, S. M. L., & Sousa, W. P. (2008). Environmental drivers in mangrove establishment and early development: A review. *Aquatic Botany*, 89(2), 105–127. <https://doi.org/10.1016/j.aquabot.2007.12.014>
- Kaufmann, R. K., Zhou, L., Myneni, R. B., Tucker, C. J., Slayback, D., Shabanov, N. V., & Pinzon, J. (2003). The effect of vegetation on surface temperature: A statistical analysis of NDVI and climate data. *Geophysical research letters*, 30(22), Article 2147. <https://doi.org/10.1029/2003GL018251>
- Kauffman, J. B., & Bhomia, R. K. (2017). Ecosystem carbon stocks of mangroves across broad environmental gradients in West-Central Africa: global and regional comparisons. *PLoS One*, 12, Article e0187749. <https://doi.org/10.1371/journal.pone.0187749>
- Kumar, A., Bhatia, A., Fagodiya, R., Malyan, S., & Meena, B. (2017). Eddy covariance flux tower: A promising technique for greenhouse gases measurement. *Advances in Plants & Agriculture Research*, 7(4), 337–340. <https://doi.org/10.15406/apar.2017.07.00263>
- Kumar, T., & Das, P. K. (2023). Estimation of gross primary productivity of Indian Sundarbans mangrove forests using field measurements and Landsat 8 Operational Land Imager data. *Tropical Ecology*, 64(1), 167-179. <https://doi.org/10.1007/s42965-022-00256-8>
- Lukman, A. H., Hidayat, M. F., Sugara, A., & Arief, M. C. W. (2022). Mangroves composition, biomass, carbon stock and their role in the climate change mitigation in Bengkulu City, Indonesia. *AAFL Bioflux*, 15(4), 1975–1988.
- Li, L., Wu, X., & Liu, S. (2015). Characteristics of photosynthesis and photosynthetic carbon fixation capacity of five mangrove tree species in Zhanjiang City. *Guangxi Zhiwu/Guihaia*, 35(6), 825-832.
- Macreadie, P. I., Costa, M. D., Atwood, T. B., Friess, D. A., Kelleway, J. J., Kennedy, H., Lovelock, C. E., Serrano, O., & Duarte, C. M. (2021). Blue carbon as a natural climate solution. *Nature Reviews Earth & Environment*, 2(12), 826-839. <https://doi.org/10.1038/s43017-021-00224-1>
- Markiet, V., & Möttus, M. (2020). Estimation of boreal forest floor reflectance from airborne hyperspectral data of coniferous forests. *Remote Sensing of Environment*, 249, Article 112018. <https://doi.org/10.1016/j.rse.2020.112018>

- Mengis, N., Paul, A., & Fernández-Méndez, M. (2023). Counting (on) blue carbon - Challenges and ways forward for carbon accounting of ecosystem-based carbon removal in marine environments. *PLOS Climate*, 2(8), Article e0000148. <https://doi.org/10.1371/journal.pclm.0000148>
- Nemani, R. R., Keeling, C. D., Hashimoto, H., Jolly, W. M., Piper, S. C., Tucker, C. J., Myneni, R. B., & Running, S. W. (2003). Climate-driven increases in global terrestrial net primary production from 1982 to 1999. *Science*, 300(5625), 1560-1563. <https://doi.org/10.1126/science.1082750>
- Nguyen, H. H., Nghia, N. H., Nguyen, H. T. T., Le, A. T., Tran, L. T. N., Duong, L. V. K., Bohm, S., & Furniss, M. J. (2020). Classification methods for mapping mangrove extents and drivers of change in Thanh Hoa province, Vietnam during 2005-2018. *Forest and Society*, 4(1), 225–242. <https://doi.org/10.24259/fs.v4i1.9295>
- Nuarsa, W., As-Syakur, A. R., Gunadi, I. G. A., & Sukewijaya, I. M. (2018). Changes in gross primary production (GPP) over the past two decades due to land use conversion in a tourism city. *ISPRS International Journal of Geo-Information*, 7(2), Article 57. <https://doi.org/10.3390/ijgi7020057>
- Paramanik, S., Varghese, R., Behera, M. D., Barnwal, S., Behera, S. K., & Bhattayacharya, B. K. (2022). Photosynthetic variables estimation in a mangrove forest. In P. C. Pandey & P. Arellano (Eds.), *Advances in Remote Sensing for Forest Monitoring* (pp. 126-149). John Wiley & Sons Ltd. <https://doi.org/10.1002/9781119788157.ch6>
- Peddinti, S. R., Kambhammettu, B. V. N. P., Rodda, S. R., Thumaty, K. C., & Suradhaniwar, S. (2020). Dynamics of ecosystem water use efficiency in citrus orchards of Central India using eddy covariance and landsat measurements. *Ecosystems*, 23(3), 511–528. <https://doi.org/10.1007/s10021-019-00416-3>
- Perissi, I., & Jones, A. (2022). Investigating European Union decarbonization strategies: Evaluating the pathway to carbon neutrality by 2050. *Sustainability*, 14(8), Article 4728. <https://doi.org/10.3390/su14084728>
- Pricillia, C. C., Patria, M. P., & Herdiansyah, H. (2021). Environmental conditions to support blue carbon storage in mangrove forest: A case study in the mangrove forest, nusa lembongan, bali, indonesia. *Biodiversitas*, 22(6), 3304–3314. <https://doi.org/10.13057/biodiv/d220636>
- Quisthoudt, K., Schmitz, N., Randin, C. F., Dahdouh-Guebas, F., Robert, E. M., & Koedam, N. (2012). Temperature variation among mangrove latitudinal range limits worldwide. *Trees*, 26, 1919-1931. <https://doi.org/10.1007/s00468-012-0760-1>
- Rafique, R., Zhao, F., De Jong, R., Zeng, N., & Asrar, G. R. (2016). Global and regional variability and change in terrestrial ecosystems net primary production and NDVI: A model-data comparison. *Remote Sensing*, 8(3), Article 177. <https://doi.org/10.3390/rs8030177>
- Raich, J. W. (1991). Potential net primary productivity in South America: Application of a global model. *Ecological Applications*, 1(4), 399–429. <https://doi.org/10.2307/1941899>
- Raj, R., Bayat, B., Lukeš, P., Šigut, L., & Homolová, L. (2020). Analyzing daily estimation of forest gross primary production based on harmonized landsat-8 and sentinel-2 product using scope process-based model. *Remote Sensing*, 12(22), 1–23. <https://doi.org/10.3390/rs12223773>
- Razali, S. M., Nuruddin, A. A., & Kamarudin, N. (2020). Mapping mangrove density for conservation of the RAMSAR site in Peninsular Malaysia. *International Journal of Conservation Science*, 11(1), 153-164.

- Reef, R., & Lovelock, C. E. (2015). Regulation of water balance in mangroves. *Annals of Botany*, 115(3), 385–395. <https://doi.org/10.1093/aob/mcu174>
- Rodda, S. R., Thumaty, K. C., Jha, C. S., & Dadhwal, V. K. (2016). Seasonal variations of carbon dioxide, water vapor and energy fluxes in tropical Indian mangroves. *Forests*, 7(2), Article 35. <https://doi.org/10.3390/f7020035>
- Shirkey, G., John, R., Chen, J., Dahlin, K., Abraha, M., Sciusco, P., Lei, C., & Reed, D. E. (2022). Fine resolution remote sensing spectra improves estimates of gross primary production of croplands. *Agricultural and Forest Meteorology*, 326, Article 109175. <https://doi.org/10.1016/j.agrformet.2022.109175>
- Suardana, A. A. M. A. P., Anggraini, N., Nandika, M. R., Aziz, K., As-Syakur, A. R., Ulfa, A., Wijaya, A. D., Prasetyo, W., Winarso, G., & Dimiyati, R. D. (2023). Estimation and mapping above-ground mangrove carbon stock using Sentinel-2 data derived vegetation indices in Benoa Bay of Bali Province, Indonesia. *Forest and Society*, 7(1), 116–134. <https://doi.org/10.24259/fs.v7i1.22062>
- Tang, Y., Li, T., Yang, X. Q., Chao, Q., Wang, C., Lai, D. Y. F., Liu, J., Zhu, X., Zhao, X., Fan, X., Zhang, Y., Hu, Q., & Qin, Z. (2023). Mango-GPP: A process-based model for simulating gross primary productivity of mangrove ecosystems. *Journal of Advances in Modeling Earth Systems*, 15(12), Article e2023MS003714. <https://doi.org/10.1029/2023MS003714>
- Trissanti, V. N., Amalo, L. F., Handayani, L. D. W., Nugroho, D., Yuliani, A. R., & Mulyana, D. (2022). The estimation of biomass and carbon stocks in mangrove forest ecosystem of Karawang Regency, West Java. In *IOP Conference Series: Earth and Environmental Science* (Vol. 1109, No. 1, p. 012099). IOP Publishing. <https://doi.org/10.1088/1755-1315/1109/1/012099>
- Turner, D., Ritts, W. D., Cohen, W. B., Gower, S. H., Zhao, M., Running, S. W., Wofsky, S., Urbansky, S., Dunn, A. D., & Munger, J. (2003). Scaling Gross Primary Production (GPP) over boreal and deciduous forest landscapes in support of MODIS GPP product validation. *Remote Sensing of Environment*, 88(1), 256–270. <https://doi.org/10.1016/j.rse.2003.06.005>
- Wang, X., Ma, M., Huang, G., Veroustraete, F., Zhang, Z., Song, Y., & Tan, J. (2012). Vegetation primary production estimation at maize and alpine meadow over the Heihe River Basin, China. *International Journal of Applied Earth Observation and Geoinformation*, 17(1), 94–101. <https://doi.org/10.1016/j.jag.2011.09.009>
- Wang, M., Cao, W., Guan, Q., Wu, G., & Wang, F. (2018). Assessing changes of mangrove forest in a coastal region of southeast China using multi-temporal satellite images. *Estuarine, Coastal and Shelf Science*, 207, 283–292. <https://doi.org/10.1016/j.ecss.2018.04.021>
- Wang, L., Jia, M., Yin, D., & Tian, J. (2019). A review of remote sensing for mangrove forests: 1956–2018. *Remote Sensing of Environment*, 231, Article 111223. <https://doi.org/10.1016/j.rse.2019.111223>
- Wang, H., Li, Z., Cao, L., Feng, R., & Pan, Y. (2021). Response of NDVI of natural vegetation to climate changes and drought in China. *Land*, 10(9), Article 966. <https://doi.org/10.3390/land10090966>
- Xiao, X., Zhang, Q., Saleska, S., Hutyyra, L., De Camargo, P., Wofsy, S., Frohling, S., Boles, S., Keller, M., & Moore, B. (2005). Satellite-based modeling of gross primary production in a seasonally moist tropical evergreen forest. *Remote Sensing of Environment*, 94(1), 105–122. <https://doi.org/10.1016/j.rse.2004.08.015>

- Xiao, X., Hollinger, D., Aber, J., Goltz, M., Davidson, E. A., Zhang, Q., & Moore III, B. (2004). Satellite-based modeling of gross primary production in an evergreen needleleaf forest. *Remote Sensing of Environment*, 89(4), 519-534. <https://doi.org/10.1016/j.rse.2003.11.008>
- Yoro, K. O., & Daramola, M. O. (2020). CO₂ emission sources, greenhouse gases, and the global warming effect. In M. R. Rahimpour, M. Farsi & M. A. Makarem (Eds.), *Advances in Carbon Capture* (pp. 3-28). Woodhead Publishing. <https://doi.org/10.1016/B978-0-12-819657-1.00001-3>
- Zaitunah, A., Meliani, S., Syahputra, O. K., Budiharta, S., Susilowati, A., Rambe, R & Azhar, I. (2021). Mapping of mangrove forest tree density using Sentinel 2A satellite image in remained natural mangrove forest of Sumatra eastern coastal. In *IOP Conference Series: Earth and Environmental Science* (Vol. 912, No. 1, p. 012001). IOP Publishing. <https://doi.org/10.1088/1755-1315/912/1/012001>
- Zeng, N., Jiang, K., Han, P., Hausfather, Z., Cao, J., Kirk-Davidoff, D., Ali, S., Zhou, S. (2022). The Chinese carbon-neutral goal: Challenges and prospects. *Advances in Atmospheric Sciences*, 39(8), 1229-1238. <https://doi.org/10.1007/s00376-021-1313-6>
- Zhang, Y., Hu, Z., Wang, J., Gao, X., Yang, C., Yang, F., & Wu, G. (2023). Temporal upscaling of MODIS instantaneous FAPAR improves forest gross primary productivity (GPP) simulation. *International Journal of Applied Earth Observation and Geoinformation*, 121, Article 103360. <https://doi.org/10.1016/j.jag.2023.103360>
- Zhang, Z., Guo, J., Jin, S., & Han, S. (2023). Improving the ability of PRI in light use efficiency estimation by distinguishing sunlit and shaded leaves in rice canopy. *International Journal of Remote Sensing*, 44(18), 5755-5767. <https://doi.org/10.1080/01431161.2023.2252165>
- Zhao, C., & Qin, C. Z. (2020). 10-m-resolution mangrove maps of China derived from multi-source and multi-temporal satellite observations. *ISPRS Journal of Photogrammetry and Remote Sensing*, 169, 389-405. <https://doi.org/10.1016/j.isprsjprs.2020.10.001>
- Zhao, D., Zhang, Y., Wang, J., Zhen, J., Shen, Z., Xiang, K & Wu, G. (2023). Spatiotemporal dynamics and geo-environmental factors influencing mangrove gross primary productivity during 2000–2020 in Gaoqiao Mangrove Reserve, China. *Forest Ecosystems*, 10, Article 100137. <https://doi.org/10.1016/j.fecs.2023.100137>
- Zheng, Y., & Takeuchi, W. (2021). *Improving Remote Sensing-Based Estimation of Mangrove Forest Gross Primary Production by Quantifying Environmental Stressors: Sea Surface Temperature, Salinity, and Photosynthetic Active Radiation*. Research Square.
- Zheng, Y., & Takeuchi, W. (2022). Estimating mangrove forest gross primary production by quantifying environmental stressors in the coastal area. *Scientific Reports*, 12(1), Article 2238.
- Zhu, X., Hou, Y., Zhang, Y., Lu, X., Liu, Z., & Weng, Q. (2021). Potential of sun-induced chlorophyll fluorescence for indicating mangrove canopy photosynthesis. *Journal of Geophysical Research: Biogeosciences*, 126(4), Article e2020JG006159. <https://doi.org/10.1029/2020JG006159>